

Siemens Logo Here

LEHRSTUHL FÜR HOCHFREQUENZTECHNIK
TECHNISCHE UNIVERSITÄT MÜNCHEN
PROF. DR.-ING. THOMAS EIBERT



Master's Thesis

Object Classification based on Micro-Doppler Signatures

Alexis González Argüello

Munich, 30-10-2017

Faculty:	Electro- und Informationstechnik
Matriculation Number:	03640751
Reviewer:	Prof. Dr.-Ing. Thomas Eibert
Supervisor:	M. Sc. Dipl.-Ing. Dominic Berges
Beginning of the Thesis:	01-10-2017
End of the Thesis:	30-10-2017

Sperrvermerk

Declaration of Authorship

Dedicated to..

Contents

1. Introduction	1
2. Radar Fundamentals	3
2.1. Radar Definitions	3
2.2. MIMO Array	4
2.3. Signal Model	4
2.4. Ranging	6
2.5. Doppler Ranging	6
2.6. Azimuth Estimation	6
2.7. Detection Theory	6
3. Clustering	7
4. Multi-Target Tracking	9
4.1. State Variable Representation of an LTI System	9
4.2. The Kalman Filter	10
4.3. Gating Techniques	10
4.4. The Assignment Problem	10
4.4.1. NN-approach	10
4.4.2. PDA-approach	10
4.4.3. JPDA-approach	10
4.5. Track Life Stages	10
4.6. Maneuver Detection and Adaptive Filtering	10
5. Micro-Doppler Signatures	11
6. Classification	13
7. Results	15
8. Summary and Outlook	17
Appendix A. Symbols and Constants	19
Appendix B. Mathematical Formulas	21

1. Introduction

2. Radar Fundamentals

Due to its wide spectrum of applications, radar systems have become important measurement instruments since the last century.

This introductory chapter is organized as follows. Section 2.1 explains the basic terminology used in the scientific community of radars. Section 2.3 presents a simple signal model used to explain the signal processing steps that take place to estimate the range (2.4) and doppler-range (2.5) of targets

2.1. Radar Definitions

Range

$$R = \frac{c_0 \Delta t}{2} \quad (2.1)$$

Pulse repetition interval (PRI)

$$f_r = \frac{1}{T} \quad (2.2)$$

Maximum unambiguous range R_u

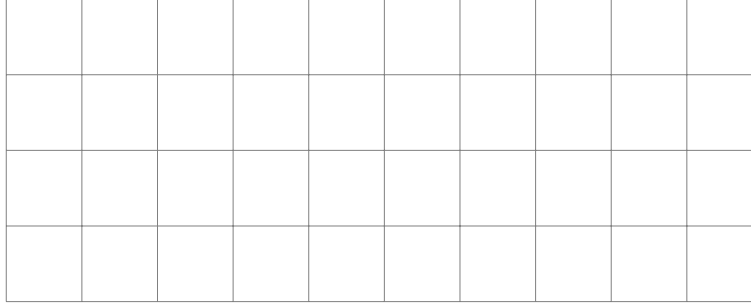


Figure 2.1.: Illustrating the unambiguous range

$$R_u = c_0 \frac{T}{2} = \frac{c_0}{2f_r} \quad (2.3)$$

Range resolution ΔR , distance between R_{max} and R_{min} divided into M range bins.

$$M = \frac{R_{max} - R_{min}}{\Delta R} \quad (2.4)$$

$$\Delta R = \frac{c_0 \tau}{2} = \frac{c_0}{2B} \quad (2.5)$$

Doppler frequency

$$f_d = \frac{2v \cos \theta}{c_0} f_0 = \frac{2v \cos \theta}{\lambda} \quad (2.6)$$

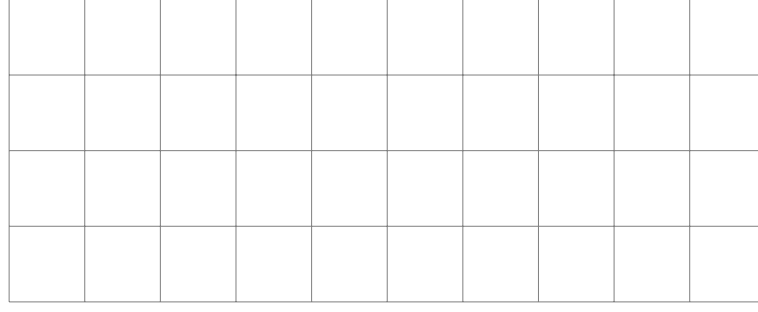


Figure 2.2.: Illustrating the doppler frequency

2.2. MIMO Array

A Multiple-Input Multiple-Output (MIMO) setup for this research has been chosen. The concepts behind the MIMO radar will be presented briefly in this section.

As the name implies, a MIMO radar consists of multiple transmit (TX) antennas and receive (RX) antennas. Given M_t transmit and M_r receive elements in an array, $M_t \times M_r$ propagation channels are obtained. This, with only $M_t M_r$ antenna elements. Furthermore, a method to define the diversity of the TX channels is required. This can be achieved by employing time division multiplexing, frequency division multiplexing, spatial coding, and orthogonal waveforms [1].

Each of the $M_t \times M_r$ propagation channels are modeled together as a virtually form array. Each element in the virtual array is placed at

$$\mathbf{x}_{ij} = (\mathbf{x}_i^{Tx} + \mathbf{x}_j^{Rx})/2, \quad (2.7)$$

where \mathbf{x}_i^{Tx} is the position of the i -TX element and \mathbf{x}_j^{Rx} of the j -RX element, as shown in fig. 2.3

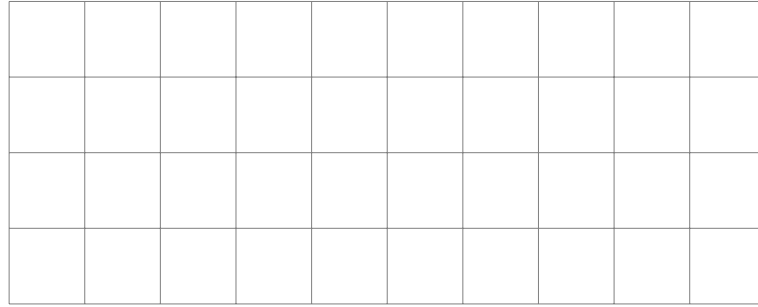


Figure 2.3.: MIMO-array

If the far-field condition is met for a given scatterer at position \mathbf{p} , the signal propagation path from a given TX element to the scatterer, plus the reflection path back to an RX element can be approximated as

$$P_{ij}(\mathbf{p}) = |\mathbf{p} - \mathbf{x}_i^{Tx}| + |\mathbf{p} - \mathbf{x}_j^{Rx}| \approx 2|\mathbf{p} - \mathbf{x}_{ij}| \quad (2.8)$$

2.3. Signal Model

For the following analyses a Frequency-Modulated Continuous-Wave (FMCW) Radar is taken into consideration. The TX array elements transmit a FMCW chirp signal, that can be modeled in as

$$s_T(t) = \exp[j(2\pi f_c t + \pi k t^2)], \quad (2.9)$$

for $-T_c/2 \leq t \leq T_c/2$, where T_c is the chirp duration, f_c the carrier frequency and the chirp rate k is defined by

$$k = \pm B/T_c. \quad (2.10)$$

Under far-field condition, the return delay between a virtual element at x_{ij} and a scatterer is given by

$$\Delta t_{ij} = \frac{2R}{c_0} + \frac{2x_{ij} \sin \theta}{c_0}, \quad (2.11)$$

where R and θ describe the location of the scatterer, R being the rang and θ the angle with respect to boresight. The received signal

$$s_R^{ij}(t) = A s_t(t - \Delta t_{ij}) \quad (2.12)$$

After the signal is received, it is down-converted by multiplying it with a replica of the transmitted signal. After low-pass filtering, the processed signal can be modeled as

$$u_{ij}(t) = s_R^{ij} s_T(t) = A \exp[j(2\pi k \Delta t_{ij} t - \pi k \Delta t_{ij}^2 + 2\pi f_c \Delta t_{ij})] \quad (2.13)$$

The sampled form of the intermediate frequency (IF) signal given N samples can be expressed as

$$u_{ij}[n] = A \exp[j(\phi + 2\pi \Psi_R n)], \quad (2.14)$$

with $\Psi_R = k \Delta t_{ij} \frac{T_c}{N}$, the normalized frequency containing the range information and $\phi = -\pi k \Delta t_{ij}^2 + 2\pi f_c \Delta t_{ij}$ contains the phase information. This expression can be generalized to MIMO radar, with M targets either static or dynamic, for the k -th observation interval by

$$u_k[n, n_C, n_A] = \sum_{m=0}^M A_m \exp[j2\pi(\phi_m + \Psi_{R,m} n + \Psi_{D,m} n_C + \Psi_{\theta,m} n_A)] + w[n, n_C, n_A] \quad (2.15)$$

where $\Psi_D = \frac{2T_c f_0}{c_0} v_R$ and $\Psi_\theta = \sin(\theta)/2$ are the normalized frequencies containing the information about range-rate and azimuth. Moreover, $w[n, n_C, n_A]$ is the present additive white Gaussian measurement noise. The parameters n , n_C and n_A represent which, sample chirp and antenna is being taken into account. Please note that ϕ_m does not correspond to ϕ .

The information collected from eq. (2.15) is usually arrange into a three-dimensional data cube as presented in fig. 2.4. Here the dimensions correspond to sample number, transmit-receive channel and chirp number.

Figure 2.4.: Data Cube

In order to estimate the spectrum of the received signal and so to determine the unknown parameters R , v_R and θ for a given target, usually a three-dimensional Fast Fourier Transform (FFT) is applied to the IF signal

$$\hat{P}_k(\Psi_R, \Psi_D, \Psi_\theta) = \sum_n \sum_{n_C} \sum_{n_A} a_R[n] a_D[n_C] a_\theta[n_A] u_k[n, n_A, n_C] \times \exp(-j2\pi\Psi_R n) \exp(-j2\pi\Psi_D n_C) \exp(-j2\pi\Psi_\theta n_A), \quad (2.16)$$

however, this usually results in a bad estimation for the azimuth range. Specifics of the signal processing will be described in the following sections.

2.4. Ranging

2.5. Doppler Ranging

2.6. Azimuth Estimation

2.7. Detection Theory

3. Clustering

4. Multi-Target Tracking

After a correct detection and clustering of targets, the detections have to be assigned to tracks which are to be updated over time. In this case, it is done to create a history of each of the target's range, azimuth angle and Doppler velocity. In a further step, the Micro-Doppler signature can be extracted from each of the tracks and be used as an input for the classifiers. More over, by keeping track of the measurements corresponding to each track, one can produce an estimate of future positions of the target, which result into a more accurate measurement of the targets position. This process is called Multi-Target Tracking (MTT).

Each track of a MTT-algorithm contains a Kalman Filter (section 4.2) which is a commonly used filter to predict future states and to calculate variables that cannot be measured directly. At each step, gating (section 4.3) is applied to each of the new detections to reduce the scope of detections that can be assigned to a given track at each time step k . After gating, the detections calculated in a given step are assigned to each of the tracks. For this, the assignment problem has to be solved (section 4.4). After the assignment has been done, the state of each of the tracks is updated according to pre-established rules (section 4.5). The whole process used for the MTT is illustrated in fig. 4.1. Given that usually a constant-velocity model is assumed, a special model needs to be

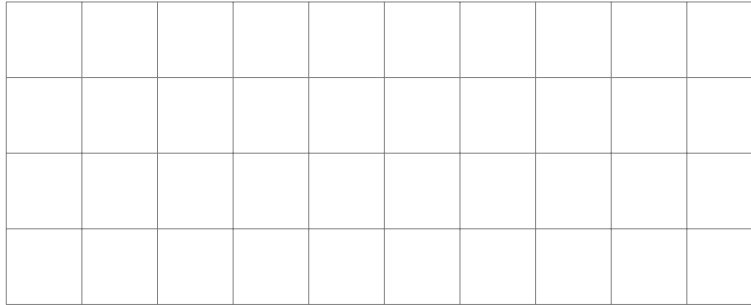


Figure 4.1.: MTT-process

implemented to consider the cases where the target has an (unknown) acceleration. This issue is handled in section 4.6.

4.1. State Variable Representation of an LTI System

A Linear Time Invariant (LTI) system can be described by by three variables, input, output and the state variable. In the case of radar, the state can be design to contain several attributes of single targets measured by the radar such as range, range-rate and azimuth angle. Since we desire to determines a target's position and velocity in Cartesian coordinates, the state vector

$$\mathbf{x} = \begin{bmatrix} x \\ y \\ v_x \\ v_y \end{bmatrix}, \quad (4.1)$$

has been chosen. The continuous-time linear system can then be written as

$$\dot{\mathbf{x}}(t) = \mathbf{A}(t)\mathbf{x}(t) + \mathbf{B}(t)\mathbf{u}(t) + \tilde{\mathbf{v}}(t), \quad (4.2)$$

where t represents time and

\mathbf{x} is the state vector of dimension n_x and $\dot{\mathbf{x}}$ its time derivative.

\mathbf{u} is the input(or control) vector of dimension n_u

$\tilde{\mathbf{v}}$ is the process noise

\mathbf{A}, \mathbf{B} are known matrices of dimensions $n_x \times n_x$ and $n_x \times n_u$

4.2. The Kalman Filter

4.3. Gating Techniques

4.4. The Assignment Problem

4.4.1. NN-approach

4.4.2. PDA-approach

4.4.3. JPDA-approach

4.5. Track Life Stages

4.6. Maneuver Detection and Adaptive Filtering

5. Micro-Doppler Signatures

6. Classification

7. Results

8. Summary and Outlook

A. Symbols and Constants

General

\oint Integration over a closed curve

Latin alphabet

B	Bandwith
f_0	Center Frequency
f_d	Doppler Frequency
f_r	Pulse Repetition Frequency (PRF)
R	Range
R_u	Unambiguous Range
T	Pulse Repetition Interval (PRI)
v	Target Velocity

Greek alphabet

ΔR	Range Resolution
ΔT	Delay
λ	wavelength
τ	Pulse Width

Constants

c_0 = 299729458 m/s

B. Mathematical Formulas

Bibliography

- [1] Yanchuan Huang, Paul Victor Brennan, Dave Patrick, I. Weller, Peters Roberts, and K. Hughes. FMCW Based MIMO Imaging Radar for Maritime Navigation. *Progress In Electromagnetics Research*, 115:327–342, 2011.